

An unified minimum effective model of magnetism in iron-based superconductors

Jiangping Hu,^{1,2,*} Bao Xu,¹ Wuming Liu,¹ Ning-Ning Hao,¹ and Yupeng Wang¹

¹*Beijing National Laboratory for Condensed Matter Physics and Institute of Physics,
Chinese Academy of Sciences, P. O. Box 603, Beijing 100190, China*

²*Department of Physics, Purdue University, West Lafayette, Indiana 47907, USA*

Since 2008, many new families of iron-based high temperature (high- T_c) superconductors have been discovered [1–4]. Unlike all parent compounds of cuprates that share a common antiferromagnetically (AF) ordered ground state, those of iron-based superconductors exhibit many different AF ordered ground states, including collinear-AF (CAF) state in ferropnictides [5], bicollinear-AF (BCAF) state in 11-ferrochalcogenide $FeTe$ [6, 7], and block-AF (BAF) state in 122-ferrochalcogenide $K_{0.8}Fe_{1.6}Se_2$ [8]. While the universal presence of antiferromagnetism suggests that superconductivity is strongly interrelated with magnetism, the diversity of the AF ordered states obscures their interplay. Here we show that all magnetic phases can be unified within an effective magnetic model. This model captures three incommensurate magnetic phases, two of which have been observed experimentally. The model characterizes the nature of phase transitions between the different magnetic phases and explains a variety of magnetic properties, such as spin-wave spectra and electronic nematicity. Most importantly, by unifying the understanding of magnetism, we cast new insight on the key ingredients of magnetic interactions which are critical to the occurrence of superconductivity.

The iron-based superconductors can be divided into two major classes, ferropnictides and ferrochalcogenides. Superconductivity in both classes, like cuprates, arises from electron- or hole-doping of their AF parent compounds. Hence, determining magnetic interactions in the parent compounds is extremely important in the identification of key magnetic interactions relevant to the development of superconductivity.

However, because of the diversity of the magnetic orders and the fact that the magnetic properties exhibit the dichotomic behavior of both local moment and itinerant electron aspects, it has been extremely difficult to find a consistent magnetic model to describe the magnetism of iron-based superconductors. Theoretically, magnetism can be explained by either local moment models where local spins interact with each other or itinerant electron models where magnetic order arises from nested Fermi surfaces. The former is appropriate for insulating materials such as the parent compounds of cuprates while the latter is suitable for metallic systems, such as chromium. However, the iron-based superconductors include rather diversified materials whose parent compounds can have either metallic or insulating ground states. More

specifically, the parent compounds of ferropnictides are bad metal [1] while the newly discovered 122-ferrochalcogenide, $K_{0.8}Fe_{1.6}Se_2$ is a block AF insulator [8]. Moreover, it was shown that even in the insulating parent compounds, itinerant electron aspects have to be included [10] and in the metallic parent compounds, local moment aspects are manifested [11]. Such a dichotomy of the magnetic properties [10–16] leads to many diversified viewpoints on what is the proper model to describe the magnetism [17–22].

In ferropnictides, the CAF state as shown in fig1(b), in principle, can be explained by Fermi surface nesting between hole pockets at Γ and electron pockets at X [23] because they are connected by the CAF ordered wavevector $Q_{CAF} = (0, \pi)$ in unfolded reciprocal space. However, the mechanism fails to explain the BCAF and BAF states shown in fig1(c,d). In these two cases, no matching Fermi pockets can be connected with their ordered wavevectors $Q_{BCAF} = (\pi/2, \pi/2)$ and $Q_{BAF} = (3\pi/5, \pi/5)$. Within a local moment picture, the CAF state can be naturally obtained in a Heisenberg model with nearest neighbor (NN) J_1 and next nearest neighbor (NNN) J_2 magnetic exchange interactions if $J_2 > |J_1|/2$ [17–19]. However, this model is quantitatively incompatible with the large anisotropy of the NN exchange interactions along the ferromagnetic (FM) and AF directions in the CAF state determined in neutron scattering experiments [11]. Intriguingly, recent neutron experiments in ferrochalcogenides show that the similar large NN anisotropy exists in both BAF[12] and BCAF states [10]. Moreover, there is almost no anisotropy between the NNN exchange interactions even though the magnetic configurations along the two NNN coupling directions in both states are different [10, 12] as shown in fig1(c,d). Two completely different solutions backed by electronic structure calculations have been proposed to solve the incompatibility in ferropnictides: one emphasizes orbital order [24–26] and the other suggests biquadratic spin interaction terms [20]. However, both solutions are inadequate in understanding the BAF and BCAF phases. For example, electronic structure calculations and orbital ordering mechanism also suggested an large NNN anisotropy in ferropnictides [27, 28], which is inconsistent with experimental results [10, 12].

Here we attempt to formulate a minimum effective spin model that unites the description of the magnetic properties of the parent compounds of the different classes of iron-based superconductors. The model has to preserve the tetragonal lattice symmetry so that it is capable of providing us the detailed relations between different magnetically ordered states as consequences of spontaneous symmetry breaking at low temperature. The model should be able to capture all the magnetically ordered ground states observed in iron-based superconductors, to explain their correct spin-wave spectra

*Electronic address: jphu@iphy.ac.cn/hu4@purdue.edu

and the anisotropy of magnetic exchange interactions, and to predict possible new states including incommensurate magnetic states. In the following, we will show by including the NN biquadratic interaction term as proposed in ref.[20], but not the NNN biquadratic interaction term, and the next next nearest neighbor (NNNN) AF Heisenberg interactions J_3 [29, 30] in $J_1 - J_2 - J_c$ model [18], we can fulfill above requirements.

Model Hamiltonian We start with the following general Hamiltonian,

$$H = \sum_{ij,n} [J_{ij} \vec{S}_{i,n} \cdot \vec{S}_{j,n} - K_{ij} (\vec{S}_{i,n} \cdot \vec{S}_{j,n})^2] + J_c \sum_{i,n} \vec{S}_{i,n} \cdot \vec{S}_{i,n+1} \quad (1)$$

where J_{ij} describe in-plane magnetic exchange interactions, J_c is inter-plane magnetic coupling along c-axis (between iron layers) and K_{ij} are in-plane non-Heisenberg biquadratic couplings. In the minimum model proposed here, we choose non-vanishing $J_{ij} = J_1, J_2$ or J_3 if and only if i, j are two NN, NNN, or NNNN sites respectively and $K_{ij} = K$ if and only if i, j are two NN sites. The interactions are sketched in fig1(a) by the dashed lines.

We note that the model is a natural extension of models in ref.[18, 20, 29, 30] proposed for ferropnictides and ferrochalcogenides before. However, all previous models only describe particular family and fail to provide a comprehensive understanding of different magnetic states.

Exact Classical Phase Diagram The classical phase diagram of the model can be obtained exactly. In fig2, we draw a typical phase diagram in the $J_3/|J_1| - J_2/|J_1|$ plane by taking $KS^2/|J_1| = 0.2$. The phase diagram is almost symmetric between $J_1 > 0$ (the right part of fig2) and $J_1 < 0$ (the left part of fig2). For $J_1 > 0$, there are three commensurate phases labeled as AFM, CAF and BCAF in fig2, which exactly describe the static magnetic states of the parent compounds of cuprates, ferropnictides and 11-ferrochalcogenide *FeTe* respectively. There are also two incommensurate phases sandwiched between the commensurate phases with ordered incommensurate wavevectors (q, π) or (π, q) (labeled as IC1) and (q, q) (labeled as IC3) respectively. The static (q, q) phase was observed in *Fe_{1+y}Te* when $y > 0.1$ [6]. Although no static (q, π) phase has been detected, the (q, π) incommensurate spin fluctuations have been observed in *FeTe_{1-x}Se_x* [31, 32], electron-overdoped *Ba(Fe_{1-x}Co_x)₂As₂* [33], and hole-doped *KFe₂As₂* [34]. If J_1 is switched to negative, namely ferromagnetic (FM), the AFM phase becomes a FM phase and (q, π) becomes $(q, 0)$ or $(0, q)$ (labeled as IC2).

More specifically, we can determine phase transition boundary. We scale other parameters with J_1 as $\tilde{K} = KS^2/J_1$, $\tilde{J}_2 = J_2/J_1$, and $\tilde{J}_3 = J_3/J_1$ for simplicity. The phase boundary between the BCAF and the (q, π) incommensurate phase is determined by $4(\tilde{J}_3 - \frac{1}{4})^2 - (\tilde{J}_2 - \frac{1}{2})^2 = (\tilde{K} - \frac{1}{2})^2$ which defines the upper branch of a hyperbolic curve centered at $(\tilde{J}_2, \tilde{J}_3) = (1/2, 1/4)$. The phase boundary between the AFM and BCAF phases is determined by $\tilde{J}_3 = -\frac{1}{2}\tilde{J}_2 + \frac{1}{2}$ and that between BCAF and CAF phases is determined by $\tilde{J}_3 = \frac{1}{2}\tilde{J}_2$. The incommensurate states appear only when

Material	Phases	(Q_x, Q_y)	J_1S	J_2S	J_3S	KS^2	J_cS
<i>CaFe₂As₂</i>	CAF	$(0, 1)\pi$	22	19	-	14	5
<i>BaFe₂As₂</i>	CAF	$(0, 1)\pi$	25	14	-	17	2
<i>FeTe</i>	BCAF	$(\frac{1}{2}, \frac{1}{2})\pi$	-34	18.5	9.5	9	-
<i>K_{0.8}Fe_{1.6}Se₂</i>	BAF	$(\frac{3}{5}, \frac{1}{5})\pi$	-10	16	9	12	1.4

TABLE I: The values of the magnetic exchange interactions in $J_1 - J_2 - J_3 - K$ model obtained from the experimental results of different parent compounds of iron-based superconductors [10–12, 16].

$\tilde{K} < 0.5$. We emphasize that finite positive $\tilde{K} > (1.5 - \sqrt{2})$ and $\tilde{J}_3 > 0.25$ are necessary conditions for the appearance of the BCAF phase. The incommensurate wavevectors of the three incommensurate phases can also be explicitly determined: (1) $(q, 0)$ or $(0, q)$ phase with $q = \arccos \frac{2\tilde{J}_2+1}{2\tilde{K}}$; (2) (q, π) or (π, q) with $q = \arccos \frac{1-2\tilde{J}_2}{2\tilde{K}}$; and (3) (q, q) with $q = \arccos \frac{1}{2(\tilde{J}_2-\lambda)}$, where $\lambda = \tilde{K} - 2\tilde{J}_3$.

Commensurate Phases The model captures three commensurate phases: AFM, CAF and BCAF. In these commensurate phases, the biquadratic interaction term effectively creates the anisotropy of the NN magnetic exchange interactions by taking a meanfield decoupling [20]. Depending on the spin alignment of two NN sites, $J_{1a} = J_1 + 2KS^2$ if it is AF and $J_{1b} = J_1 - 2KS^2$ if it is FM. Therefore, effectively, our model becomes a $J_{1a} - J_{1b} - J_2 - J_3 - J_c$ model in these phases. Experimentally, the spin wave excitations in the parent compounds, *CaFe₂As₂* [11] and *BaFe₂As₂* [16], were fitted well to the $J_{1a} - J_{1b} - J_2 - J_c$ model, and those of *FeTe* was fitted well to a $J_{1a} - J_{1b} - J_2 - J_3 - J_c$ model [12].

More interestingly, in the ferrochalcogenide *K_{0.8}Fe_{1.6}Se₂*, featuring intrinsic vacancy ordering, the fitting of spin wave excitations to a $J_{1a} - J_{1b} - J_2 - J'_2 - J_3$ model has concluded a large FM J_{1a} , AF J_{1b} and very small anisotropy between two AF NNN couplings J_2 and J'_2 [10]. Our model hence successfully describes the magnetism of this new material as well. The presence of vacancy ordering does not drastically affect the magnetic interactions. Instead, it reduces the magnetic frustration to stabilize the BAF order [35].

From the experimental results of spin wave excitations [10–12, 16], we now can extract the magnetic exchange parameters of our model for different parent compounds. The results are summarized in Table1. We note that FeTe is near the boundary of the BCAF phase and incommensurate phases. The values listed in Table1 is within the error bar of experimental values in [12]. This table displays a central message that all iron based superconductors share a similar AF NNN exchange interaction J_2 . However the sign of J_1 is different between ferropnictides and ferrochalcogenides and a significant AF J_3 exists in ferrochalcogenides but not in ferropnictides.

Spin Excitations in Incommensurate Phases The model also predicts three incommensurate phases. We can calculate the distinct features of spin excitations in these three phases. The typical spin excitation spectra in the three incommensurate phases as the function of wavevectors δ are shown in

fig3(a)-(f). In general, spin excitations include two branches, which can be identified as an acoustic mode and an optical mode. In the (π, q) phase, the two modes connect with each other at two new incommensurate positions $\delta = \pm q_0$ when the wavevector (π, δ) varies as shown fig3(a). If we calculate the intensity of these spin wave excitations measured by neutron scattering, an hour-glass like behavior along this direction becomes prominent at low energy as shown in fig4. This behavior has been recently reported in *FeSe_{0.4}Te_{0.6}*[36] and a clear explanation was not given before. The dispersion along (δ, π) as varying δ has much larger energy dispersion than the one along (π, δ) and reaches maximum at (π, π) which is consistent with experimental results observed in ref.[31] as shown in fig3(b). In $(0, q)$ phase, the dispersion of spin excitations along $(0, \delta)$ as varying δ is very similar to the one along (δ, π) in (π, q) phase as shown in fig3(c) and that along $(\delta, 0)$ is similar to the one along (π, δ) as shown in fig3(d). In the (q, q) phase, the two spin wave modes connect at $(0, \pi)$ point as shown in fig3(e,f) and fig3(g,h), displaying a Dirac-type dispersion. The two modes has much larger energy separation in the case of $J_1 > 0$ (shown in

fig3(e,f)) than $J_1 < 0$ (shown in fig3(g,h). More detailed spin wave properties are included in supplement materials. These distinct features can be used to determine the effective magnetic exchange couplings even if the incommensurate order is not static.

Nematism and Effective Field Theory Both the CAF and BCAF states break the C^4 rotational symmetry of the tetragonal lattice. The rotational symmetry breaking can be separately described by an Ising or nematic order as shown in ref.[18, 19]. Without the specific biquadratic term K , when the parameters of the $J_1 - J_2 - J_c$ model are fixed in the CAF phase region, a weak biquadratic term can be developed through the ‘order by disorder’ mechanism [18, 19, 37] and the nematic phase transition can take place at a transition temperature T_N higher than the CAF transition temperature T_c if the inter-layer coupling J_c is much weaker than J_2 [18]. This physics can be analytically described in the continuum limit. As show in ref.[18], the effective field theory of the $J_1 - J_2 - J_c$ model in the continuum limit is given by

$$H_{CAF} = \int d^2\mathbf{r} \sum_{n,\alpha} \left[\frac{1}{2} J_2 |\nabla \vec{\phi}_{n,\alpha}(\mathbf{r})|^2 - J_c \vec{\phi}_{n,\alpha}(\mathbf{r}) \cdot \vec{\phi}_{n+1,\alpha}(\mathbf{r}) \right] - g \sum_n \left[\vec{\phi}_{n,1}(\mathbf{r}) \cdot \vec{\phi}_{n,2}(\mathbf{r}) \right]^2 + J_1 \sum_n \vec{\phi}_{n,1}(\mathbf{r}) \partial_x \partial_y \vec{\phi}_{n,2}(\mathbf{r}), \quad (2)$$

where we use the same notions as ref. [18]: $\vec{\phi}_{n,\alpha=1,2}$ specify the two AF Neel orders in the two sublattices of the tetragonal lattice shown in fig1(a) (for simplicity, we take $S = 1$ in this section). The nematic order is defined to be $\sigma = 2g \langle \vec{\phi}_{n,1}(\mathbf{r}) \cdot \vec{\phi}_{n,2}(\mathbf{r}) \rangle$. Without the biquadratic term K , $g \sim 0.13J_1^2/J_2$. With this term, we just need to modify $g \sim 0.13J_1^2/J_2 + K$. Therefore, the calculations and the results in ref. [18] are still valid. The large g value due to the spe-

cific biquadratic K term simply enhances the nematic order and increases the temperature range of spin nematic fluctuation above T_N , which has been observed experimentally[16].

In the case of BCAF states, the similar effective model for $J_1 - J_2 - J_3$ model has also been derived in ref.[38]. Including J_c , the effective field theory of the $J_1 - J_2 - J_3 - J_c$ model close to the BCAF states can be written as

$$H_{BCAF} = \int d^2\mathbf{r} \sum_{n,\alpha} \left[\frac{1}{2} J_3 |\nabla \vec{\phi}_{n,\alpha}(\mathbf{r})|^2 - J_c \vec{\phi}_{n,\alpha}(\mathbf{r}) \cdot \vec{\phi}_{n+1,\alpha}(\mathbf{r}) \right] - g' \sum_n \{ [\vec{\phi}_{n,1}(\mathbf{r}) \cdot \vec{\phi}_{n,3}(\mathbf{r})]^2 + [\vec{\phi}_{n,2}(\mathbf{r}) \cdot \vec{\phi}_{n,4}(\mathbf{r})]^2 \} - J_1 \int d^2\mathbf{r} \sum_n \left[\vec{\phi}_{n,1}(\mathbf{r}) \cdot \nabla_x \vec{\phi}_{n,2}(\mathbf{r}) + \vec{\phi}_{n,4}(\mathbf{r}) \cdot \nabla_x \vec{\phi}_{n,3}(\mathbf{r}) - \vec{\phi}_{n,2}(\mathbf{r}) \cdot \nabla_y \vec{\phi}_{n,3}(\mathbf{r}) - \vec{\phi}_{n,1}(\mathbf{r}) \cdot \nabla_y \vec{\phi}_{n,4}(\mathbf{r}) \right] \quad (3)$$

where $\vec{\phi}_{n,\alpha}$ with $\alpha = 1, 2, 3, 4$ are four Neel order parameters defined in the four sublattices of the tetragonal lattice specified by the J_3 coupling and $g' \sim 0.13J_2^2/J_3$. Differing from

the case of the CAF, the biquadratic term in the case of the BCAF adds an additional coupling term into above effective Hamiltonian, which is given by

$$H_K = -K \int d^2\mathbf{r} \sum_n \{ [\vec{\phi}_{n,1}(\mathbf{r}) \cdot \vec{\phi}_{n,2}(\mathbf{r})]^2 + [\vec{\phi}_{n,1}(\mathbf{r}) \cdot \vec{\phi}_{n,4}(\mathbf{r})]^2 + [\vec{\phi}_{n,2}(\mathbf{r}) \cdot \vec{\phi}_{n,3}(\mathbf{r})]^2 + [\vec{\phi}_{n,3}(\mathbf{r}) \cdot \vec{\phi}_{n,4}(\mathbf{r})]^2 \} \quad (4)$$

The complete field description of the $J_1 - J_2 - J_3 - J_c - K$ model near the *BCAF* phase is given by $H_T = H_{BCAF} + H_K$. In this model, there are four independent Ising orders $\sigma_1 = g' \vec{\phi}_{n,1}(\mathbf{r}) \cdot \vec{\phi}_{n,3}(\mathbf{r})$, $\sigma_2 = g' \vec{\phi}_{n,2}(\mathbf{r}) \cdot \vec{\phi}_{n,4}(\mathbf{r})$, $\sigma_+ = K(\vec{\phi}_{n,1}(\mathbf{r}) + \vec{\phi}_{n,3}(\mathbf{r})) \cdot (\vec{\phi}_{n,2}(\mathbf{r}) + \vec{\phi}_{n,4}(\mathbf{r}))$ and $\sigma_- = K(\vec{\phi}_{n,1}(\mathbf{r}) - \vec{\phi}_{n,3}(\mathbf{r})) \cdot (\vec{\phi}_{n,2}(\mathbf{r}) - \vec{\phi}_{n,4}(\mathbf{r}))$. A detailed study of this effective field model will be present elsewhere. Here, we simply discuss the case when K is much larger than g' to demonstrate that the effective field model indeed captures phase transitions. In this case, the transition between the *BCAF* state and the (q, q) incommensurate state is controlled by the Ising order σ_+ . It is easy to show that when $|\sigma_+|$ is large, the ground state is the *BCAF* state. The transition takes place at $|\sigma_c| = \frac{J_2^2}{4J_3^2}$. When $|\sigma_+| < |\sigma_c|$, the model is in an incommensurate (q, q) state with $q = \frac{2}{J_1}(|\sigma_c| - |\sigma_+|)$.

Discussion By describing the magnetism of the different parent compounds of iron based superconductors in a single effective magnetic model, we can cast new insight on the microscopic origin of magnetism. From the magnetic exchange coupling parameters of the effective model, it is very clear that the magnetism is neither purely local nor purely itinerant, rather it is a complicated mix of the two. The presence of significant NNNN coupling J_3 suggests the local exchange mechanisms such as superexchange or double exchange are not enough to account for all magnetic exchange interactions. Moreover, the sign change of J_1 between ferropnictides and ferrochalcogenides suggests that the NN exchange interactions are sensitive to subtle difference in band structures. However, the robustness of NNN J_2 interactions indicates that the NNN J_2 coupling is most likely determined by local superexchange mechanism. In ref.[20], the authors suggest that the NN biquadratic term K in ferropnictides stems from the strong magnetostructural coupling. However, this explanation does not provide an understanding of the absence of NNN biquadratic term in the *BCAF* state of *FeTe* since the lattice distortion in *FeTe* is monoclinic rather than orthorhombic as in ferropnictides[6]. More throughout studies of the origin of the biquadratic term are needed.

The model reveals the significant difference between ferropnictides and ferrochalcogenides: the sign difference of J_1 and the large AF J_3 in ferrochalcogenides. These significant differences may suggest the importance of the p orbitals of As

or *Te/Se* on the influence of magnetism. So far, most theoretical models are constructed based on the d orbitals of irons with onsite interactions. Since the effect of electron-electron correlations is believed to be weaker in ferropnictides than in ferrochalcogenides, one would expect the range of magnetic interactions should be shorter in ferrochalcogenides than in ferropnictides, which contradicts the existence of large J_3 interactions in ferrochalcogenides but not in ferropnictides. This contradictory can be resolved if the significant parts of magnetic exchange interactions are generated through the p -orbitals of As or Se/Te. The effective magnetic exchange interactions obtained from onsite electron-electron interactions are not enough to account for entire magnetic exchange couplings. This also explains that why magnetism is so sensitive to the distance of As or Se/Te away from iron planes [39] because the distance may strongly affect the mixture of p orbitals in electronic structure.

The model, as an effective low energy model of magnetism, also tells us the power and limitation of LDA calculations performed for iron-based superconductors where the effect of electron-electron correlation can not be ignored. Without any doubt, the LDA calculations explain many magnetic properties in iron-based superconductors. For ferropnictides, the LDA results of J_{1a} , J_{1b} and J_2 values are in a good agreement with experiments [22]. However, LDA calculation wrongly predicted the large anisotropy of J_2 in the *BCAF* and *BAF* states [27, 28]. This failure is not surprising since the LDA in magnetically ordered state is simply a complicated meanfield approach.

It has been shown that the high energy magnetic excitations in electron-doped ferropnictides are very similar to those of parent compounds[40]. This proves that the short range magnetic correlations in superconducting states are still dominated by the magnetic exchange interactions determined in the corresponding parent compounds. The doping destroys the long range magnetic correlation but not the short range interactions. Especially, the J_2 magnetic exchange interactions should be expected to vary little against doping. In *FeTe_{1-x}Se_x*, the incommensurate spin excitations are rather robust against the replacement of Te by Se[31, 32]. This fact suggests that J_3 is relatively stable against the replacement in this family of materials as well. Therefore, if AF exchange couplings are responsible for superconductivity, we expect both J_2 and J_3 plays a significant role in superconductivity of ferrochalcogenides.

-
- [1] Kamihara, Y., Watanabe, T., Hirano, M. & Hosono, H. Iron-Based Layered Superconductor $\text{La}[\text{O}_{1-x}\text{F}_x]\text{FeAs}$ ($x = 0.05-0.12$) with $T_c = 26$ K. *J. Am. Chem. Soc.* 130, 3296-3297 (2008).
- [2] Chen, X. H., Wu, T., Wu, G., Liu, R. H., Chen, H. & Fang, D. F. Superconductivity at 43K in $\text{SmFeAsO}_{1-x}\text{F}_x$. *Nature* 453, 761-762 (2008).
- [3] Hsu, F. C. *et al.* Superconductivity in the PbO-type structure α -FeSe. *Proc. Natl. Acad. Sci. USA* 105, 14262-14264 (2008).
- [4] Guo, J. *et al.* Superconductivity in the iron selenide $\text{K}_x\text{Fe}_2\text{Se}_2$. *Phys. Rev. B* 82, 180520 (2010).
- [5] de la Cruz, C. *et al.* Magnetic order close to superconductivity in the iron-based layered $\text{LaO}_{1-x}\text{F}_x\text{FeAs}$ systems. *Nature* 453, 899-902 (2008).
- [6] Bao, W. *et al.* Tunable (π, π) -type antiferromagnetic order in α -Fe(Te,Se) superconductors. *Phys. Rev. Lett.* 102, 247001 (2009).
- [7] Li, S. *et al.* First-order magnetic and structural phase transitions in $\text{Fe}_{1+y}\text{Se}_x\text{Te}_{1-x}$. *Phys. Rev. B* 79, 054503 (2009).
- [8] Bao, W. *et al.* A Novel Large Moment Antiferromagnetic Order

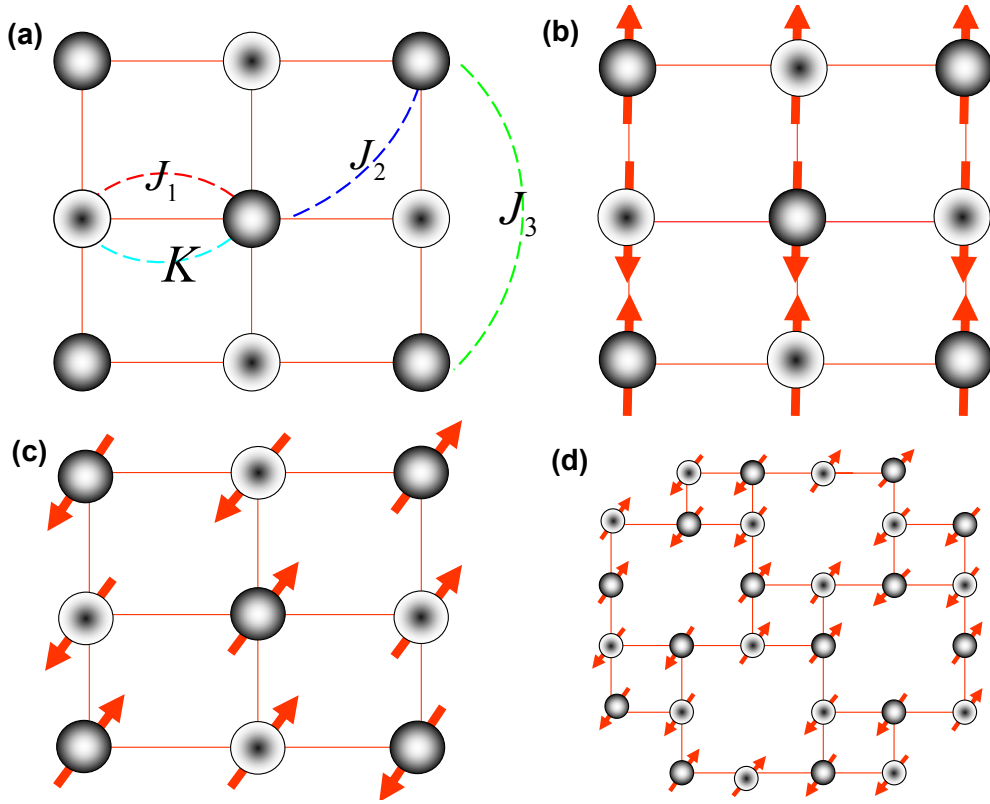


FIG. 1: (a). The sketch of magnetic interaction parameters of $J_1 - J_2 - J_3 - K$. (b) The collinear-antiferromagnetic state (CAF) in ironpnictides, for example CaFe_2As_2 . (c) The bicollinear-antiferromagnetic state (BCAF) in FeTe . (d) The block-antiferromagnetic state (BAF) with $\sqrt{5} \times \sqrt{5}$ vacancy ordering in $\text{K}_{0.8}\text{Fe}_{1.6}\text{Se}_2$.

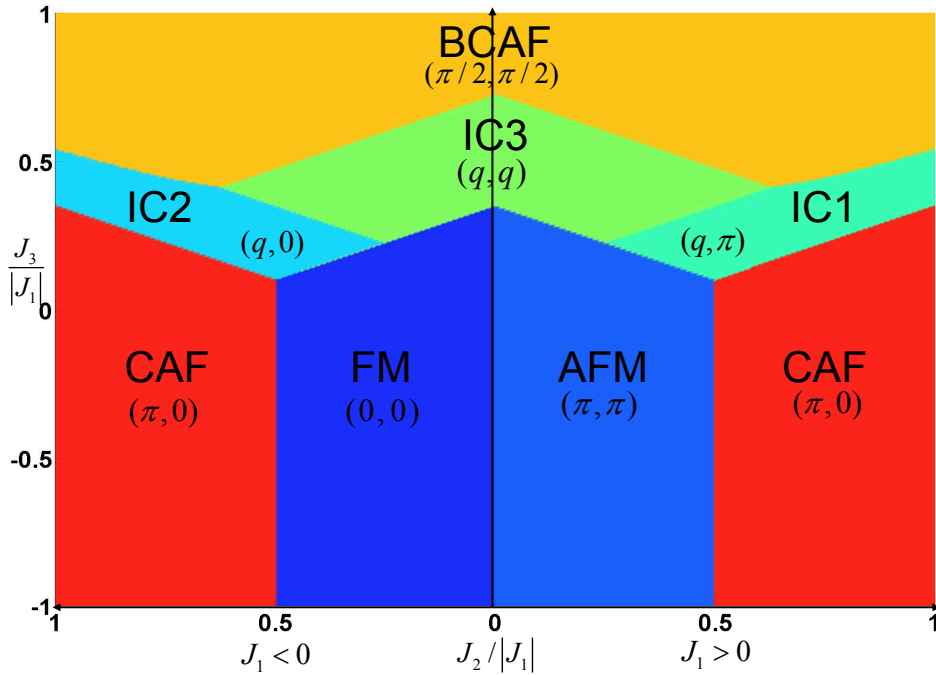


FIG. 2: The classical phase diagram of the $J_1 - J_2 - J_3 - K$ model at $K = 0.2J_1$. There are total four commensurate and three incommensurate magnetic phases. Their labels and the ordered wavevectors are specified in the figure.

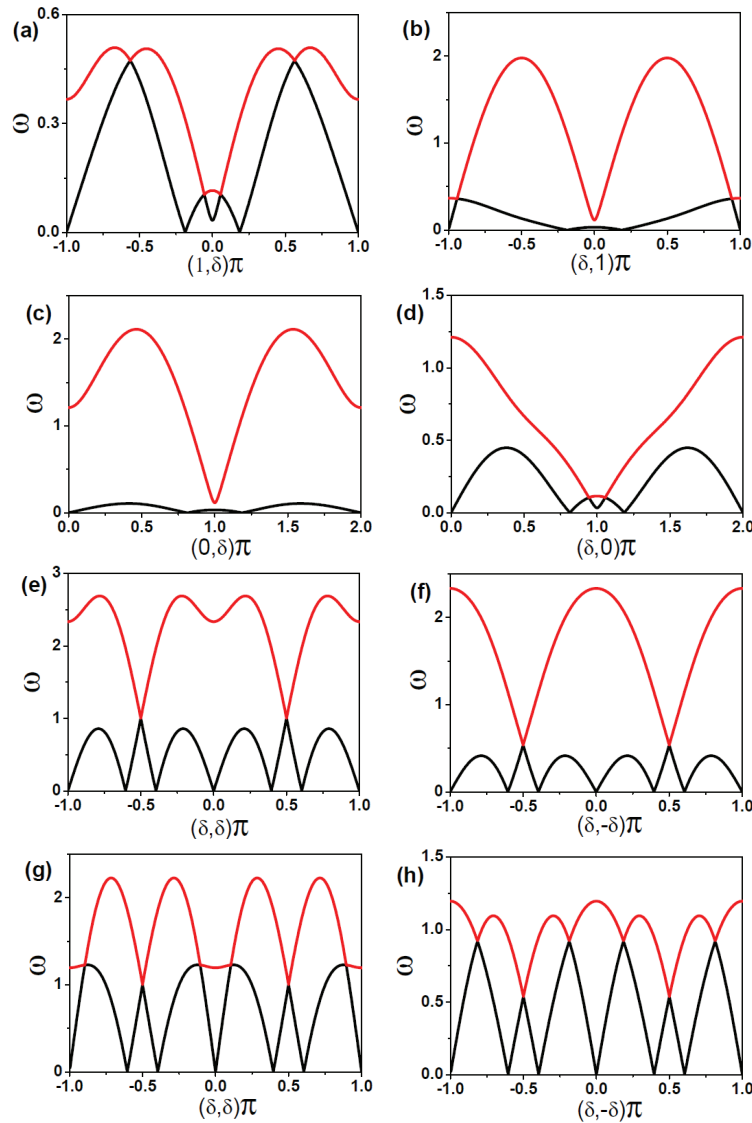


FIG. 3: The spin waves in incommensurate phases: (a) along $(1, \delta)\pi$ and (b) along $(\delta, 1)\pi$ in the (π, q) phase, (c) along $(0, \delta)\pi$ and (d) along $(\delta, 0)\pi$ in the $(0, q)$ phase, and (e)/(g) along $(\delta, \delta)\pi$ and (f)/(h) along $(\delta, -\delta)\pi$ in the (q, q) -phase. The parameters are fitted to be $S = 1$, $(J_1, J_2/|J_1|, J_3/|J_1|, KS^2/|J_1|) = (1, 0.6, 0.06, 0)$ in (a) and (b), $(-1, 0.6, 0.06, 0)$ in (c) and (d), $(-1, 0.6, 0.5, 0.05)$ in (e) and (f), and $(1, 0.6, 0.5, 0.05)$ in (g) and (h).

in $K_{0.8}Fe_{1.6}Se_2$ Superconductor. Arxiv: 1102.0830 (2011).

- [9] Ying, J. J. *et al.* Superconductivity and Magnetic Properties of high-quality single crystals of $A_xFe_2Se_2$ ($A = K$ and Cs). Arxiv: 1012.5552 (2010).
- [10] Wang, M. *et al.* Spin Waves and Magnetic Exchange Interactions in Insulating $Rb_{0.89}Fe_{1.58}Se_2$. Arxiv: 1105.4675 (2011).
- [11] Zhao, J. *et al.* Spin Waves and Magnetic Exchange Interactions in $CaFe_2As_2$. Nature Physics 5, 555-560 (2009).
- [12] Lipscombe, O.J. *et al.* Spin waves in the $(\pi, 0)$ magnetically ordered iron chalcogenide $Fe_{1.05}Te$, Phys. Rev. Lett. 106 057004(2011).
- [13] Diallo, S. O. *et al.* Itinerant magnetic excitations in antiferromagnetic $CaFe_2As_2$. Phys. Rev. Lett. 102, 187206 (2009).
- [14] Matan, K, Morinaga, R., Iida, K., and Sato, T. J. Anisotropic itinerant magnetism and spin fluctuations in $BaFe_2As_2$: A neutron scattering study. Phys. Rev. B 79, 054526 (2009).
- [15] Yang L.X., *et al.* Electronic structure and exotic exchange splitting in spin-density-wave states of $BaFe_2As_2$. Phys. Rev. Lett. 102, 107002 (2009).
- [16] Harriger, L. W. *et al.*, Nematic spin fluid in the tetragonal phase of $BaFe_2As_2$. arXiv:1011.3711.
- [17] Si, Q., and Abrahams, E., Strong correlations and magnetic frustration in the high T_c iron pnictides. Phys. Rev. Lett. 101, 076401 (2008).
- [18] Fang, C., Yao, H., Tsai, W. F., Hu, J. P. and Kivelson, S. A. Theory of electron nematic order in $LaOFeAs$. Phys. Rev. B 77, 224509 (2008).
- [19] Xu, C. K., Muller, M. and Sachdev, S. Ising and spin orders in iron-based superconductors. Phys. Rev. B 78, 020501(R) (2008).

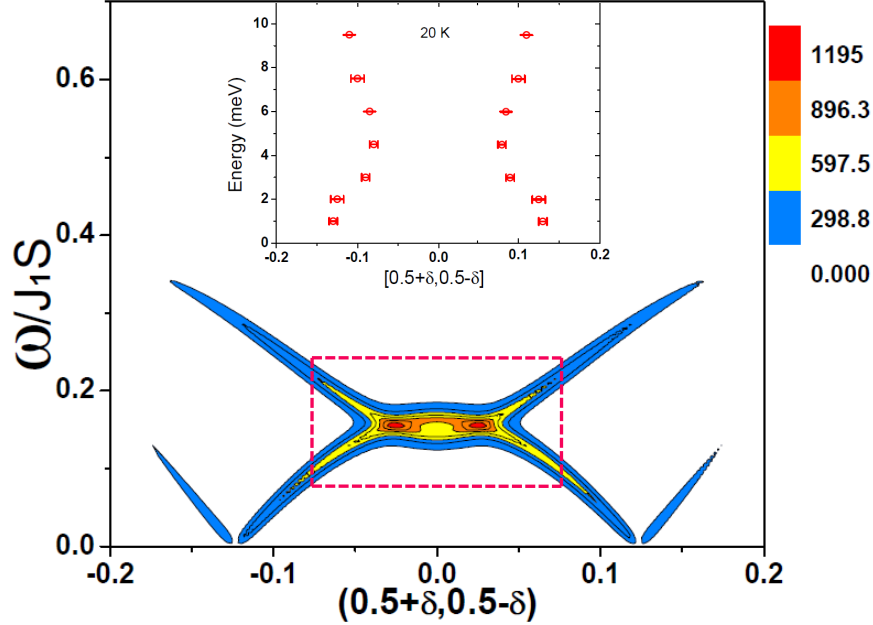


FIG. 4: The hour-glass-like spin waves along $(1/2 + \delta, 1/2 - \delta)_T$ in the (π, q) phase. The parameters are set to $(J_1S, J_2/J_1, J_3/J_1, KS^2/J_1) = (30, 0.55, 0.045, 0.02)$. The inset depicts the experimental results released in Ref.[36]. The observed region is labeled by the dashed lines.

- [20] Wysocki, A. L. Belashchenko K. D. and Antropov V. P. Consistent Model of Magnetism in Ferropnictides. *Nature Physics*, 7 485 (2011).
- [21] Mazin, I. I. and Johannes, M. D. A key role for unusual spin dynamics in ferropnictides. *Nature Physics* 5, 14115 (2009).
- [22] Han, M. J., Yin, Q., Pickett, W. E. and Savrasov, S. Y. Anisotropy, itinerancy, and magnetic frustration in high- T_c iron pnictides. *Phys. Rev. Lett.* 102, 107003 (2009)
- [23] Dong J., *et al.* Competing Orders and Spin-Density-Wave Instability in $\text{La}(\text{O}_{1-x}\text{F}_x)\text{FeAs}$. *Europhysics Lett.* 83, 27006 (2008).
- [24] Lv, W. C., Kroger, F., and Phillips, P., Orbital ordering and unfrustrated $(\pi, 0)$ magnetism from degenerate double exchange in iron pnictides. *Phys. Rev. B* 82, 045125 (2010).
- [25] Lee, C.-C., Yin, W.-G., and Ku, W. Ferro-orbital order and strong magnetic anisotropy in the parent compounds of iron-pnictide superconductors. *Phys. Rev. Lett.* 103, 267001 (2009).
- [26] Turner A. M., Wang F. and Vishwanath A. Kinetic Magnetism and Orbital Order in Iron Telluride. *Phys. Rev. B* 80, 224504 (2009).
- [27] M. J. Han and S. Y. Savrasov, *Phys. Rev. Lett.* 103, 067001 (2009).
- [28] Cao, C. and Dai, J., Block Spin Ground State and 3- Dimensionality of $(K, Tl)\text{Fe}_{1.6}\text{Se}_2$. arXiv: 1102.1344.
- [29] Ma F. *et al.* Bi-collinear antiferromagnetic order in the tetragonal α -FeTe. *Phys. Rev. Lett.* 102 177003 (2009),
- [30] Fang C., Bernevig A. B., and Hu J, Theory of Magnetic Order in $\text{Fe}_{1+y}\text{Te}_{1-x}\text{Se}_x$. *Phys. Lett.* 86, 67005 (2009).
- [31] Lumsden M. D. *et al.* Evolution of spin excitations into the superconducting state in $\text{FeTe}_{1-x}\text{Se}_x$. *Nature Phys.* 6, 182 (2010).
- [32] Argyriou D. N. *et al.*, Incommensurate itinerant antiferromagnetic excitations and spin resonance in the $\text{FeTe}_{0.6}\text{Se}_{0.4}$ superconductor. *Phys. Rev. B* 81, 220503(R) (2010).
- [33] Pratt D. K. *et al.* Incommensurate spin-density wave order in electron-doped BaFe_2As_2 superconductors. arXiv:1104.0717 (2011).
- [34] Lee, S-H. *et al.*, Incommensurate spin fluctuations in hole-overdoped superconductor KFe_2As_2 , *Phys. Rev. Lett.* 106, 067003 (2011).
- [35] Fang, C. *et al.* Magnetic frustration and iron-vacancy ordering in iron chalcogenide. arXiv:1103.4599v2.
- [36] Li S. *et al.* Hour-glass dispersion in spin excitations of superconducting $\text{FeSe}_{0.4}\text{Te}_{0.6}$. *Phys. Rev. Lett.* 105,157002 (2010).
- [37] Chandra P., Coleman P. and Larkin A. J., Ising transition in frustrated Heisenberg models. *Phys. Rev. Lett.* 64, 88(1990).
- [38] Xu Cenke and Hu JP, Field theory for magnetic and lattice structure properties of $\text{Fe}_{1+y}\text{Te}_{1-x}\text{Se}_x$, arXiv:0903.4477 (2009).
- [39] Kuroki K. *et al.* Pnictogen height as a possible switch between *high*- T_c nodeless and *low*- T_c nodal pairings in the iron based superconductors. *Phys. Rev. B* 79, 224511 (2009)
- [40] Dai P.C., Private Communications.

Author contributions J.P.H. initiates the project and the model described in this paper. J.P. H., B.X. and N.N.H. carry out the calculations in this paper. All of the authors discuss the project and are involved in writing the paper.

Acknowledgement: We are grateful to Prof. S. Kivelson, Prof. Pengcheng Dai, Prof. Donglei Feng, Prof. Hong Ding, Prof. X. H. Chen, Prof. Tao Xiang and Prof. Nanlin Wang for fruitful discussions. This work is supported in part by the National Science Foundation of China and National Basic Research Program of China (973 Program).